Available online at www.sciencedirect.com
SCIENCE DIRECT®
Journal of Molecular Structure 695–696 (2004) 287–293
Journal of MOLECULAR STRUCTURE
www.elsevier.com/locate/molstruc

Molecular structure, spectral constants, and fermi resonances in chlorine nitrate

Douglas T. Petkie[a], Rebecca A.H. Butler[b], Paul Helminger[c], Frank C. De Lucia[d,*]

[a]*Department of Physics, Wright State University, Dayton, OH 45435, USA*
[b]*Jet Propulsion Laboratory, California Institute of Technology, Pasadena, CA 91109, USA*
[c]*Department of Physics, University of South Alabama, Mobile, AL 36688, USA*
[d]*Department of Physics, 174 West 18th Ave., The Ohio State University, Columbus, OH 43210-1106, USA*

Received 31 October 2003; revised 31 October 2003; accepted 9 December 2003

Abstract

Chlorine nitrate has two low-lying vibrational modes that lead to a series of Fermi resonances in the $9^{v_9}7^{v_7}$ family of levels that include the $9^2 \Leftrightarrow 7^1$ and $9^3 \Leftrightarrow 7^1 9^1$ dyads and the $9^4 \Leftrightarrow 9^2 7^1 \Leftrightarrow 7^2$ and $9^5 \Leftrightarrow 9^3 7^1 \Leftrightarrow 9^1 7^2$ triads. These states, along with the ground and 9^1 vibrational states, have been previously analyzed with millimeter and submillimeter wave spectroscopy and provide a substantial body of data for the investigation of these resonances and their impact on calculated spectroscopic constants and structural parameters. Due to fitting indeterminacies, these previous analyses did not include the main Fermi resonance interaction term. Consequently, the fitted rotational constants are linear combinations of the unmixed rotational constants of the basis vibrational states. In this paper, we have calculated the contributions of the Fermi resonances to the observed rotational constants in a model that determines the vibrational–rotational constants, the Fermi term and the mixing between interacting vibrational states, the cubic potential constant (ϕ_{997}) that connects interacting levels through a Fermi resonance, and the inertial defects. These results agree with predictions from *ab initio* and harmonic force field calculations and provide further experimental information for the determination of the fundamental molecular properties of chlorine nitrate.

Keywords: Chlorine nitrate; Fermi resonances; Anharmonic resonances; Rotational constants; Vibration–rotation constants

1. Introduction

Infrared and microwave spectroscopy began as rather separate disciplines, each with its own science: the infrared studying vibrational physics and the microwave the rotational degrees of freedom. However, there is now considerable overlap in the information content due to the growth in resolution of infrared techniques and in sensitivity, spectral coverage, and speed of microwave techniques. These experimental advances provide the spectroscopic community with significant opportunities for the development of a unified understanding of the ro-vibrational structure of molecules. Additionally, with the increased speed, power, and availability of *ab initio* calculations, the quantum chemistry and spectroscopy communities can support each other in the determination of fundamental molecular properties.

1.1. Diatomics—fundamental Hamiltonians

Ro-vibrational spectroscopy was an early focus of molecular spectroscopy, but in the context of exploring the new subject of quantum mechanics, with molecular structure at the core. This was especially true for diatomic molecules, which were especially amenable to detailed calculation [1–4]. For example, in the context of an expansion of the intermolecular potential

$$U(\xi) = a_0\xi^2(1 + a_1\xi + a_2\xi^2 + a_3\xi^3 + \cdots)$$

Dunham obtained an explicit relation for the ro-vibrational energy levels

$$\frac{E_{vJ}}{h} = \sum_{l,m} Y_{l,m}\left(v + \frac{1}{2}\right)^l J^m(J+1)^m \quad (1)$$

and relationships among the potential constants, the $Y_{l,m}$, and the parameters, such as B_e, which described the molecular structure. Additionally, these relations were

* Corresponding author. Tel.: +614-688-4774; fax: +614-292-7557.
E-mail address: fcd@mps.ohio-state.edu (F.C. De Lucia).

0022-2860/$ - see front matter © 2003 Elsevier B.V. All rights reserved.
doi:10.1016/j.molstruc.2003.12.007

widely exploited to obtain the best molecular description from weighted least squares fit of data taken from both vibrational and rotational spectroscopy [5,6].

1.2. More complex molecules—effective Hamitonians

The construction of the more general asymmetric rotor Hamiltonian also started from structural considerations [7,8] and evolved to the general form of the vibration-rotational Hamiltonian derived by Watson [9]. Through contact transformations and perturbation theory, a reduced form of the effective rotational Hamiltonian can be determined which provides detailed expressions for the centrifugal distortion constants and the vibrational dependence of the principle rotational constants for asymmetric rotors [10,11]. This treatment provides a basic relationship for the dependence of the effective rotational constants on the vibrational quantum numbers and is given by

$$\beta_v = \beta_e - \sum_i \alpha_i^\beta (v_i + 1/2) + \sum_{j \geq i} \gamma_{ij}^\beta (v_i + 1/2)(v_j + 1/2) + \ldots \tag{2}$$

where $\beta_v = A_v, B_v, C_v$ is a rotational constant for vibrational state v, β_e is the equilibrium rotational constant, α_i^β and γ_{ij}^β are the linear and second-order vibration–rotation interaction constants, v_i and v_j are the vibrational quantum numbers and the summation indices i and j are over the normal modes of the molecule. This expression applied to the $9^{v_9}7^{v_7}$ family of levels can be written as

$$\beta_{v_9 v_7} = \beta_0 - v_9 \alpha_9^\beta + v_9(v_9 + 1)\gamma_{99}^\beta - v_7 \alpha_7^\beta \tag{3}$$

where β_0 is the ground state rotational constant and we have only included constants that were fit for in this work.

While these expressions are of the same form as the leading terms of Eq. (1), the additional complexity of the problem precluded the development of the relations between the 'rotational' and 'vibrational' terms to sufficient accuracy for combined fits to fundamental parameters. These complexities are due to the large number of normal modes, resonances between states, and differing effective Hamiltonian models that include the consideration of the Watson reduction and centrifugal distortion [11]. The net result has been the highly successful fitting of massive amounts of accurate data to effective Hamiltonians with large numbers of adjustable parameters, many of which only have a passing acquaintance with any fundamental molecular property.

1.3. Mixing and perturbations

It is often possible to accurately account even for highly mixed and perturbed spectra without explicit consideration of the perturbation. Often the effects of weak perturbations, especially those whose energy level crossings are at relatively high J, are absorbed into the rotational and distortional constants. Two states that interact via a Fermi resonance are particularly difficult to model with physical meaning due to the fitting indeterminacy between the unperturbed band origin difference and the Fermi interaction constant.

However, this indeterminacy can be lifted with explicit spectroscopic information about the mixing of the two states. A primary example is the $9^2 \Leftrightarrow 5^1$ Fermi resonance in nitric acid. In this case, the torsional splitting in the pure rotational spectrum of the 9^2 state is induced onto the 5^1 state through a Fermi resonance, allowing a direct determination of the mixing between the two states [12,13]. An additional measurement of the infrared intensity ratios between the $\nu_5 - \nu_0$ and $2\nu_9 - \nu_0$ bands reveals the same mixing ratio since the overtone band borrows intensity from the fundamental band through the same mixing mechanism [12].

However, in the case of chlorine nitrate, the torsional splitting is too small to be observed, even in the pure rotational spectra. Additionally, no detailed information on the infrared band intensities in this spectral region ($200–300\ cm^{-1}$) has been published that might be used to calculate the Fermi mixing.

Fortunately, another method of removing the fitting indeterminacy is available through a global analysis of the rotational constants. This includes the model of Eq. (3) of the vibration–rotation interaction, constrained by the interaction terms that model the mixing due to the Fermi resonances. This method is similar to those found in Townes and Schawlow [14] and Blanco et al. [15].

This paper will focus on the impact of Fermi resonances on spectroscopically determined rotational constants in the context of a series of Fermi resonances in the $9^{v_9}7^{v_7}$ family of levels in chlorine nitrate. A model is presented that uses the perturbed rotational constants determined from the several separate spectroscopic analyses and Eq. (3) to calculate the unperturbed rotational constants, the vibration–rotation parameters, and the Fermi interaction constants. From these fitted parameters and the fitted band origin differences, the cubic potential constant and the inertial defects of each state are also calculated. These results compare favorably with harmonic force field analyses and *ab initio* calculations.

2. Methods

The results of previous millimeter and submillimeter wave analyses of the ground state, 9^1, $9^2 \Leftrightarrow 7^1$ and $9^3 \Leftrightarrow 7^1 9^1$ dyads and the $9^4 \Leftrightarrow 9^2 7^1 \Leftrightarrow 7^2$ and $9^5 \Leftrightarrow 9^3 7^1 \Leftrightarrow 9^1 7^2$ triads used in the work can be found in Refs. [16–21] for the ^{35}Cl isotope. Details of each analysis can be found in the literature and the relevant aspects are summarized here. Each analysis used a Watson S-reduced

Hamiltonian in the I^r representation. The ground and 9^1 states were found not to be perturbed while the remaining dyads and triads included higher order anharmonic resonances and, in some cases, higher order Coriolis interaction terms. Each dyad/triad was fit with the philosophy of using a minimal number of spectroscopic constants while reproducing the millimeter and submillimeter wave spectrum to experimental accuracy. A fundamental fitting indeterminacy (100% correlation) between the band origin difference and the Fermi resonance term prevented the simultaneous determination of both parameters in the case of chlorine nitrate. Because of this indeterminacy and without *a priori* knowledge of the unperturbed band origins or the Fermi interaction constant (the cubic potential constant), only the difference in the perturbed band origins was fit in each analysis. Higher order anharmonic resonance interactions included in the analyses, *i.e.* those with J and K dependence or localized resonances, allowed the determination of the perturbed band origin differences in all cases but the 9^5 level, where an insufficient number of locally perturbed rotational levels were measured. Exclusion of the Fermi resonance term significantly affects the rotational and distortional constants for each state with the rotational constants being a linear combination of the unperturbed constants. Similar correlations with the rotational constants prevent the determination of the first order Coriolis interaction terms; however, neglecting this interaction term does not significantly affect the rotational constants.

To model the perturbed rotational constants, we used a method similar to the one described in Townes and Schawlow [14] and Blanco et al. [15], in which the perturbed rotational constants were corrected by fitting for a Fermi resonance constant between interacting states and modeling the vibrational dependence of the rotational constants by Eq. (3). In this model, each rotational constant $\beta_v = A_v, B_v, C_v$ of two interacting states has the same mixing parameter, as shown in the Hamiltonian block matrix of Fig. 1. The on-diagonal terms are the unperturbed rotational constants and the off-diagonal terms depend on the Fermi resonance. This mixing results in the observed rotational constants.

The effect of the Fermi resonance on the rotational constants can be derived by considering two interacting states in a 2×2 matrix that results in the mixing of the vibrational wavefuctions given by

$$\psi_1 = a\psi_1^0 + b\psi_2^0$$

$$\psi_2 = b\psi_1^0 - a\psi_2^0$$

where ψ_i and ψ_i^0 are the perturbed and unperturbed vibrational wave functions and a and b are the wavefuction coefficients describing the mixing and are related by the expression $a^2 + b^2 = 1$. This leads to an averaging of

										Δ_6	$7^2 9^1$
									Δ_5	$7^1 9^3$	Δ_6
									9^5	Δ_5	
							Δ_4	7^2			
						Δ_3	$7^1 9^2$	Δ_4			
						9^4	Δ_3				
				Δ_2	$7^1 9^1$						
				9^3	Δ_2						
		Δ_1	7^1								
		9^2	Δ_1								
	9^1										
gs											

Fig. 1. Block matrix Hamiltonian of the rotational constants due to the systematic structural ϕ_{997} Fermi resonances in chlorine nitrate. The on-diagonal terms are the rotational constants, $\beta = A, B, C$, for each respective state given by Eq. (3), and the off-diagonal Δ_i terms represent the shift in the rotational levels due to the Fermi resonances given by Eq. (4). These Fermi terms were not fit for in the original spectral analyses in Refs. [19–21].

the unperturbed rotational constants given by

$$\beta'_{v_9 v_7} = a^2 \beta_{v_9 v_7} + b^2 \beta_{v'_9 v'_7}$$

$$\beta'_{v'_9 v'_7} = b^2 \beta_{v_9 v_7} + a^2 \beta_{v'_9 v'_7}$$

where β' and β are the perturbed and unperturbed rotational constants. This mixing can be parameterized as a shift in the rotational constants expressed as

$$\Delta^{\beta}_{v'_9 v'_7 \leftrightarrow v_9 v_7} = (\beta_{v'_9 v'_7} - \beta_{v_9 v_7})(a^2_{v'_9 v'_7 \leftrightarrow v_9 v_7} - 1) \tag{4}$$

where $(\beta_{v'_9 v'_7} - \beta_{v_9 v_7})$ is the difference in the unpertubed rotational constants and $a^2_{v'_9 v'_7 \leftrightarrow v_9 v_7}$ is the fractional mixing between the two states. The fractional mixing is given by

$$a^2_{v'_9 v'_7 \leftrightarrow v_9 v_7} = \frac{1}{2}\left[1 + \left(1 + \frac{4W^2_{v'_9 v'_7 \leftrightarrow v_9 v_7}}{\Delta E^2_{v'_9 v'_7 \leftrightarrow v_9 v_7, 0}}\right)^{-\frac{1}{2}}\right] \tag{5}$$

where $\Delta E_{v'_9 v'_7 \leftrightarrow v_9 v_7, 0}$ is the unperturbed band origin difference and $W_{v'_9 v'_7 \leftrightarrow v_9 v_7}$ is the Fermi resonance term. In the limit of a large Fermi resonance, $a^2_{v'_9 v'_7 \leftrightarrow v_9 v_7} \rightarrow 1/2$ indicating a 50/50 mixing and the rotational constants of the two interacting states are averaged together to identical values.

The least squares fit of the perturbed rotational constants was made by constructing a design matrix for each rotational constant that was a function of the vibration–rotation interaction constants of Eq. (3) and the shifts in the rotational constants due to the Fermi interactions given by Eq. (4). The general expression for the perturbed rotational constant is

$$\beta'_{v_9 v_7} = \beta_0 - v_9 \alpha^{\beta}_9 + v_9(v_9 + 1)\gamma^{\beta}_{99} - v_7 \alpha^{\beta}_7 \pm \Delta^{\beta}_{v'_9 v'_7 \leftrightarrow v_9 v_7} \tag{6}$$

As an example, the equations corresponding to the $9^2 \Leftrightarrow 7^1$ dyad used in constructing the design matrix are

$$\beta'_{20} = \beta_0 - 2\alpha_9^\beta + 6\gamma_{99}^\beta + \Delta_{20\leftrightarrow 01}$$

and

$$\beta'_{01} = \beta_0 - \alpha_7^\beta - \Delta_{20\leftrightarrow 01}$$

where

$$\Delta_{02-10}^\beta = (\beta_{20} - \beta_{01})(a_{20\leftrightarrow 01}^2 - 1).$$

The Fermi resonance is given by the vibrational matrix element

$$W = \left\langle v_7, v_9 | \frac{1}{2}\phi_{799} q_9^2 q_7 | v_7 - 1, v_9 + 2 \right\rangle$$

$$= \frac{\phi_{799}}{4\sqrt{2}} \sqrt{v_7(v_9+1)(v_9+2)} \quad (7)$$

where ϕ_{799} is the cubic potential constant. While each Fermi resonance depends on the same cubic potential constant, each interaction was treated as a free parameter resulting in the index i for the above Fermi interaction parameters Δi, included in Fig. 1. The reason for the extra degrees of freedom is this fit relates back to the effective Hamiltonian models used in the previously published analyses. Due to large correlations with rotational and distortional constants, most on-diagonal Fermi resonance terms (i.e. those with $\Delta K_a = 0$) were not included in the analyses. These terms also affect the rotational constants preventing a more accurate determination of the cubic potential constant in this study.

3. Results

Table 1 shows the spectroscopically observed rotational constants, residuals of the least squares fit to equations of the form of Eq. (6) and the contribution, $\Delta^\beta_{v'_9 v'_7 \leftrightarrow v_9 v_7}$, to each rotational constant due to the mixing. Note that for each dyad or triad, the $\Delta^\beta_{v'_9 v'_7 \leftrightarrow v_9 v_7}$ contributions sum to a value close to zero. The vibration–rotation interaction and Fermi interaction parameters determined by the least squares fit to the rotational constants are given in Table 2. The linear vibration–rotational constants were determined both for the v_9 and v_7 modes for each rotational constant while the only non-linear term used was for the A rotational constant for the v_9 series of levels. Figs. 2–4 show these results graphically. It is noteworthy that at the scale of the graph the difference between the spectroscopically observed constants and those calculated by the model are very small, while in contrast, the differences between the unperturbed case represented by the line and these points are significant. Obvious residuals persist that cannot be improved upon by the inclusion of higher-order non-linear vibration–rotation interaction constant, i.e. γ_9^B or γ_9^C. This may be a result of the step- wise analysis procedure used here. In Section 4 we will discuss a more global fitting approach.

Table 1
The rotational constants used in the least squares fit to determine the vibration–rotation and Fermi interaction constants

State	Constant	Obs.–Calc.	Δ_i[a]
A rotational constant			
gs	12105.78446(768)	−0.1378	−0.1378
9^1	12004.63991(1438)	−0.1024	−0.1024
7^1	12116.8725(164)	0.1479	28.2066
9^2	11932.9734(175)	0.0655	−27.9930
$7^1 9^1$	11998.2681(138)	0.0921	−45.4175
9^3	11851.6172(41)	0.1119	45.6217
9^4	11772.9283(37)	0.0034	64.4998
$7^1 9^2$	11959.46541(253)	−0.0057	15.7553
7^2	12103.60378(35)	0.0523	−80.2050
9^5	11693.9923(203)	−0.0172	81.9265
$7^1 9^3$	11867.0666(301)	−0.0811	22.1272
$7^2 9^1$	11978.3477(289)	−0.1290	−104.2812
B rotational constant			
gs	2777.000984(1235)	0.1346	0.1346
9^1	2776.814837(1824)	−0.2907	−0.2907
7^1	2771.27229(73)	0.4760	1.3454
9^2	2776.26133(67)	−0.2140	−1.0834
$7^1 9^1$	2771.22763(43)	−0.3587	1.0615
9^3	2776.03342(301)	−0.1303	−1.5505
9^4	2775.884392(47)	0.0946	−1.9388
$7^1 9^2$	2769.996541(50)	0.0374	−0.4087
7^2	2766.01697(49)	0.5500	3.0296
9^5	2775.83434(35)	0.3821	−2.2280
$7^1 9^3$	2769.89706(61)	−0.1072	−0.7474
$7^2 9^1$	2765.90321(49)	−0.5737	2.6766
C rotational constant			
gs	2258.151052(1286)	0.2176	0.2176
9^1	2262.133054(181)	−0.3201	−0.3201
7^1	2251.95469(52)	0.5362	2.6014
9^2	2264.61104(50)	−0.2967	−2.3618
$7^1 9^1$	2256.86549(33)	−0.3811	2.9924
9^3	2267.908567(252)	−0.2105	−3.5840
9^4	2271.275128(41)	0.0927	−4.7372
$7^1 9^2$	2257.327026(44)	−0.0060	−1.0657
7^2	2247.233155(43)	0.5703	6.4600
9^5	2274.83991(34)	0.5078	−5.6922
$7^1 9^3$	2261.26121(15)	−0.1306	−1.6512
$7^2 9^1$	2252.43393(44)	−0.5795	7.1410

The rotational constants for the ^{35}Cl isotope are from the analyses Refs. [18–21] with the number in parentheses the standard deviation of the constant reported in the reference.

[a] Departure from the unperturbed vibration–rotation model due to the Fermi Resonance given by Eq. (4). Note that the sum of the differences within each dyad or triad is close to zero.

Table 3 shows the band origin differences (which were calculated in our earlier analyses of the several dyads and triads) and the mixing coefficients calculated in this work. The table also shows the Fermi matrix element coupling the vibrational levels calculated from them, and finally, the cubic potential constant determined via Eq. (7). The good agreement among these separately determined values for the cubic potential constant is gratifying.

Table 2
Fitted vibration–rotation interaction constants and mixing coefficients

Parameter	Value (MHz)
A_0	12105.92(36)
α_9^A	102.38(59)
γ_9^A	0.60(12)
α_7^A	−39.94(59)
B_0	2776.87(26)
α_9^B	−0.239(82)
α_7^B	6.94(14)
C_0	2257.93(26)
α_9^C	−4.520(84)
α_7^C	8.58(18)
$a^2_{20\leftrightarrow01}$	0.8828(23)
$a^2_{30\leftrightarrow11}$	0.8085(24)
$a^2_{40\leftrightarrow21}$	0.7259(47)
$a^2_{21\leftrightarrow02}$	0.6657(42)
$a^2_{50\leftrightarrow31}$	0.6481(58)
$a^2_{31\leftrightarrow11}$	0.5618(49)

Numbers in parentheses are one standard deviation as obtained by the least squares fit; the subscripts for the mixing coefficient represent $v_9' v_7' \leftrightarrow v_9 v_7$.

From these five values we calculated the cubic potential constant to be $\phi_{997} = 20.5 \pm 1.4\ \mathrm{cm}^{-1}$.

A second order perturbative anharmonic analysis using GAUSSIAN 03 [22] was performed at the B3LYP level with a 6-31G(d) basis set to calculate both the cubic potential and vibration–rotation interaction constants. The results of this calculation compare favourably with results from the above analysis with a direct comparison provided in Table 4. Additionally, we compared our results with predictions from two experimentally determined harmonic force field analyses. The inertial defects were calculated from the fitted rotational and vibration–rotation interaction constants and are in agreement with those calculated by Muller, et al. [18]. Orphal, el al. [23] predicted the vibration–rotation interaction constant for v_9, which is also in agreement with our fit. Both of these comparisons are also provided in Table 4.

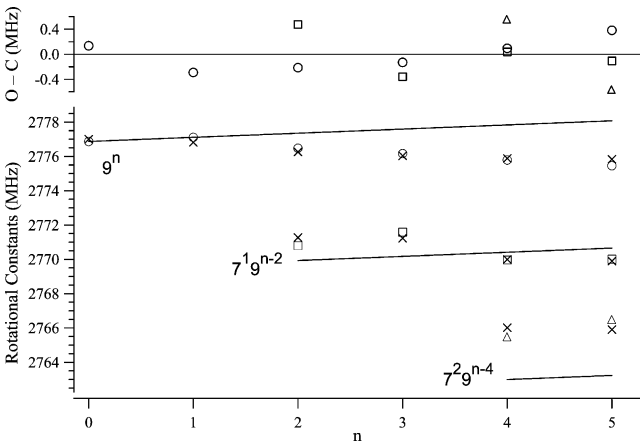

Fig. 3. The B rotational constants used in this analysis. The × are the rotational constants from the analyses in Refs. [18–21], the open circles (○) are the fitted 9^{v_9} series, the open squares (□) are the $7^1 9^{v_9}$ series of states, and the open triangles (△) are the $7^2 9^{v_9}$ series of states. The solid lines represent the behaviour of the unperturbed rotational constants (without Fermi resonances) as a function of vibrational state (or the vibrational–rotational constants). The residuals are on an expanded scale.

4. Discussion

In Section 1 we noted that for diatomic molecules not only has it been common to directly combine infrared and microwave data but to do so in the context of a unified and

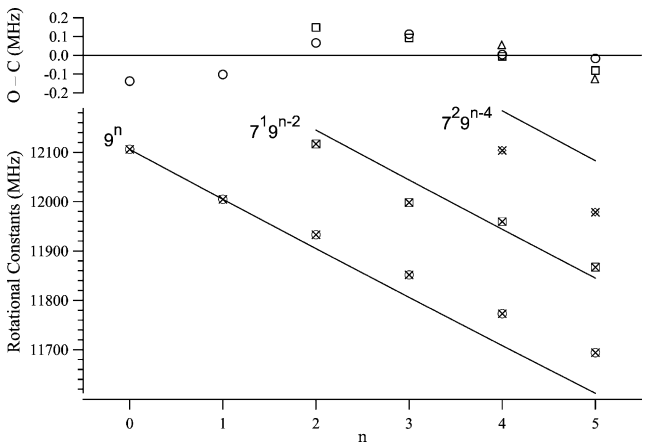

Fig. 2. The A rotational constants used in this analysis. The × are the rotational constants from the analyses in Refs. [18–21], the open circles (○) are the fitted 9^{v_9} series, the open squares (□) are the $7^1 9^{v_9}$ series of states, and the open triangles (△) are the $7^2 9^{v_9}$ series of states. The solid lines represent the behaviour of the unperturbed rotational constants (without Fermi resonances) as a function of vibrational state (or the vibrational-rotational constants). The residuals are on an expanded scale.

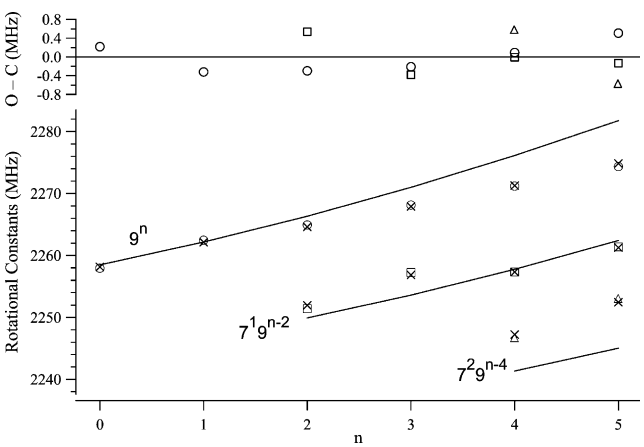

Fig. 4. The C rotational constants used in this analysis. The × are the rotational constants from the analyses in Refs. [18–21], the open circles (○) are the fitted 9^{v_9} series, the open squares (□) are the $7^1 9^{v_9}$ series of states, and the open triangles (△) are the $7^2 9^{v_9}$ series of states. The solid lines represent the behaviour of the unperturbed rotational constants (without Fermi resonances) as a function of vibrational state (or the vibrational–rotational constants). The residuals are on an expanded scale.

Table 3
Vibrational energy band differences, mixing coefficients, the calculated Fermi interaction parameters and the calculated cubic potential constant

States	ΔE (cm^{-1})[a]	a^2 (mixing)	W (cm^{-1})[b]	ϕ_{997} (cm^{-1})[c]
$9^2 \Leftrightarrow 7^1$	16.805128(26)	0.8828(23)	5.402(46)	21.61(19)
$9^3 \Leftrightarrow 7^1 9^1$	24.338505(18)	0.8085(24)	9.570(46)	22.10(11)
$9^4 \Leftrightarrow 9^2 7^1$	28.1460(12)	0.7259(47)	12.555(67)	20.50(11)
$9^2 7^1 \Leftrightarrow 7^2$	14.5727166(14)	0.6657(42)	6.874(22)	19.444(61)
$9^5 \Leftrightarrow 9^3 7^1$	–	0.6481(58)	–	–
$9^3 7^1 \Leftrightarrow 9^1 7^2$	23.2405(24)	0.5618(49)	11.531(14)	18.830(23)

[a] From Refs. [19–21] with one standard deviation uncertainties in all cases.
[b] Calculated from a^2 and ΔE using Eq. (5).
[c] Calculated from Eq. (7).

Table 4
Comparison between fitted vibration–rotation interaction constants and inertial defects with *ab initio* and harmonic force field calculations

Constant	Observed[a]	*ab initio*[b]	Predicted[c]
ϕ_{997}	±20.5(1.4)	−18.42	–
α_9^A	102.38(59)	132.36	91.1
α_9^B	−0.239(82)	−0.779	0.00
α_9^C	−4.520(84)	−3.268	−4.71[d]
α_7^A	−39.94(59)	−35.14	–
α_7^B	6.94(14)	2.85	–
α_7^C	8.58(18)	6.92	–
Δ_9	−0.702(32)	–	−0.692384
Δ_7	0.613(37)	–	0.566828

[a] Determined by the least squares fit with the inertial defects calculated using the results of Table 2; numbers in parentheses are the estimated uncertainties; ϕ_{997} was determined statistically from the results in Table 3 and the sign is not determinable.
[b] Using GAUSSIAN 03 and the B3LYP/6-31(d) method with the anharmonic force field calculation included.
[c] The inertial defect, Δ, predictions are from Ref [18] and the α predictions are from Ref. [23].
[d] The sign of α_9^C from the latter reference has been changed to account for different sign conventions used in that study [26].

coupled Hamiltonian, that these relations reduced the number of parameters required to describe the data, and that in general more reliable and stable analyses resulted. We have also noted the difficulty of developing equations analogous to the Dunham relations for more complicated molecules.

However, we have shown above that if the perturbations are properly accounted for in the Hamiltonians of interacting states, a related reduction in the number of parameters results. We have also shown that the resulting parameters are in much better agreement with the results of *ab initio* theory that are related to molecular structure and other more fundamental molecular properties but in a more numerical way than in the analytical Dunham relations. The agreement with *ab initio* calculations also provides support for the method of supplementing experimental rotational constants with vibration–rotation interaction constants calculated from *ab initio* force fields to determine the equilibrium structures as demonstrated by Groner and Warren [24] and Pawlowski, et al. [25].

A better model might be a global analysis that is inclusive of all pure rotational and ro-vibrational spectral data with the constraints of Eq. (6) placed on spectroscopic constants. For the 12 vibrational states $9^{v_9}7^{v_7}$ below $9^1 7^2$, this would be equivalent to fitting for the 16 parameters of Table 2 in place of 36 individual rotational constants.

Furthermore, if one makes the plausible argument that the fractional change in constants at all orders should be related to the fractional structural changes, consideration of Figs. 1–3 places these changes at a few percent for the rotational constants. Although strong arguments can be made against setting undeterminable high order parameters at the ground state constants in individual fits, if the perturbations which cause large variations among observed spectroscopic parameters are accounted for in the fit, then expansions of the form of Eq. (2) can be used to reduce the degrees of freedom in the fits due to centrifugal distortion as well. Indeed, since the fractional uncertainty in distortion constants is typically orders of magnitude larger for distortion constants, in many cases these expansions will have no terms.

While such reductions might a first blush seem of minor academic interest, in many real spectroscopic problems the assignment of the rotational structure in high lying states is difficult for both microwave and infrared spectroscopists. Typically, as an assignment tool one uses information from lower lying states to project the location of lines in as yet unassigned states. Although strategies vary, many are equivalent to using only the linear α_i^β terms of Eq. (2).

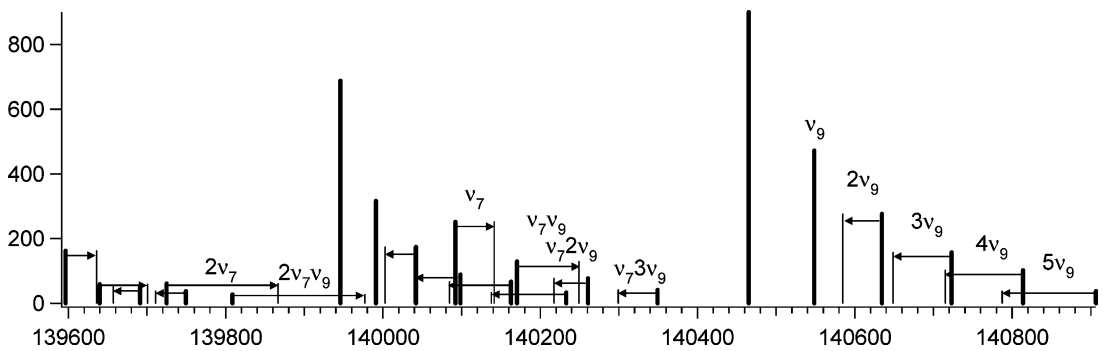

Fig. 5. Stick spectra with arrows showing the shifts induced by perturbations from the unperturbed positions (bold lines) to the observed positions (lighter lines).

Consider for example Fig. 5. The right side of the figure shows a progression of lines in the 9^{v_9} family of transitions. The arrows show the shifts from the positions calculated from the unperturbed model to the observed positions that include the effects from the Fermi resonances. These shifts are both significant and irregular. Similar shifts are shown for the $9^{v_9}7^{v_7}$ families. Thus, an understanding of the impact of these perturbations on the observed spectra is an important tool in the assignment of weak spectra in highly excited states.

5. Summary

We have used the extensive mm/submm data set of $ClONO_2$, which extends over a large number of vibrational states, to show that many of the state-to-state variations among the spectroscopically observed spectral constants arise not from fundamental structural differences, but rather from mixings induced by perturbations. We have also shown with the removal of these perturbation induced changes that reasonably 'normal' variations result and that a significant reduction in the number of parameters which describe these states is possible. Additionally, the removal of the perturbation contribution to the spectroscopic parameters substantially increases their agreement with spectroscopic parameters calculated by numerical methods from molecular structure.

Acknowledgements

We would like to acknowledge NASA and the Ohio Supercomputing Center for support of this work.

References

[1] P.M. Morse, Phys. Rev. 34 (1929) 57.
[2] J.L. Dunham, Phys. Rev. 41 (1932) 721.
[3] L. Pauling, E.B. Wilson, Introduction to Quantum Mechanics, McGraw-Hill, New York, 1935.
[4] W. Born, R. Oppenheimer, Ann. Physik 84 (1927) 457.
[5] E.F. Pearson, W. Gordy, Phys. Rev. 177 (1969) 59.
[6] F.C. De Lucia, P. Helminger, W. Gordy, Phys. Rev. A3 (1971) 1849.
[7] E.B. Wilson, J.B. Howard, J. Chem. Phys. 4 (1936) 260.
[8] B.T. Darling, D.M. Dennison, Phys. Rev. 57 (1940) 128.
[9] J.K.G. Watson, Mol. Phys. 15 (1968) 479.
[10] I.M. Mills, in: K.N. Rao, C.W. Mathews (Eds.), Vibration–Rotation Structure in Asymmetric-and Symmetric-Top Molecules, Academic Press, New York, 1972, Chapter 3.2.
[11] W. Gordy, R.L. Cook, Microwave Molecular Spectra, Wiley, New York, 1984.
[12] T.M. Goyette, C.D. Paulse, L.C. Oesterling, F.C. De Lucia, P. Helminger, J. Mol. Spectrosc. 167 (1994) 365.
[13] D.T. Petkie, T.M. Goyette, P. Helminger, H.M. Pickett, F.C. De Lucia, J. Mol. Spectrosc. 208 (2001) 121.
[14] C.H. Townes, A.L. Schawlow, Microwave Spectroscopy, McGraw-Hill Dover Publications, Inc, New York, 1955.
[15] S. Blanco, A. Lesarri, J.C. López, J.L. Alonso, A. Guarnieri, J. Mol. Spectrosc. 175 (1996) 267.
[16] R.D. Suenram, D.R. Johnson, J. Mol. Spectrsoc. 65 (1977) 239.
[17] R.D. Suenram, F.J. Lovas, J. Mol. Spectrosc. 105 (1984) 351.
[18] H.S.P. Muller, P. Helminger, S.H. Young, J. Mol. Spectrosc. 181 (1997) 363.
[19] R.A.H. Butler, S. Albert, D.T. Petkie, P. Helminger, F.C. De Lucia, J. Mol. Spectrosc. 213 (2002) 8.
[20] R.A.H. Butler, D.T. Petkie, P. Helminger, F.C. De Lucia, J. Mol. Spectrosc. 220 (2003) 150.
[21] R.A.H. Butler, D.T. Petkie, P. Helminger, F.C. De Lucia, J. Mol. Spectrosc. (2003) (in preparation).
[22] M.J. Frisch, G.W. Trucks, H.B. Schlegel, G.E. Scuseria, et al., GAUSSIAN03 (Revision B.04), Gaussian, Inc., Pittsburgh PA, 2003.
[23] J. Orphal, M. Morillon-Chapey, A. Diallo, G. Guelachvili, J. Chem. Phys. A 101 (1997) 1062.
[24] P. Groner, R.D. Warren, J. Mol. Struct. 599 (2001) 323.
[25] F. Pawlowski, P. Jørgensen, J. Olson, F. Hegelund, T. Helgaker, J. Gauss, K.L. Bak, J.F. Stanton, J. Chem. Phys. 116 (2002) 6482.
[26] J. Orphal, personal communication, 2003.